A thermionic energy converter with an electrolytically etched tungsten emitter

A thermionic energy converter with an electrolytically etched tungsten emitter

G. H. M. Gubbels and R. Metselaar
Laboratory for Solid State Chemistry and Materials Science, Eindhoven University of Technology, P.O. Box 513, 5600 MB Eindhoven, The Netherlands

(Received 8 January 1990; accepted for publication 2 May 1990)

The bare work functions of etched and unetched plasma-sprayed tungsten were found to be 4.8 and 4.5 eV, respectively. The electron emission of plasma-sprayed tungsten, both etched and unetched, was measured over a wide range of temperatures in a cesium atmosphere. Work functions were derived from the saturation current densities. In the ignited mode, current-voltage (I-V) characteristics were measured. The influence of the emitter, collector, and cesium reservoir temperatures on the I-V characteristics was investigated. Barrier indexes of 2.06 and 2.30 eV were found for etched and unetched tungsten emitters, respectively. At an emitter temperature of 1400 °C, in the case of an unetched tungsten emitter a power density of 1.5 W/cm^2 was found, while for an etched tungsten emitter it was 4.5 W/cm^2. This increased power density could be attributed to a lower collector work function. The lower cesiated collector work function resulted from the evaporation of oxygen, as WO_3, from the etched tungsten emitter.

I. INTRODUCTION

A thermionic energy converter (TEC) is a device which directly converts heat into electricity. It consists of two electrodes, one of which (the emitter) is heated to a temperature where electrons are emitted thermally. The other electrode (the collector) is kept at a lower temperature and collects the electrons. Part of the energy is removed from the emitter by evaporation of electrons, transported to the collector, and transformed into heat by condensing electrons. The remaining part is converted into electric power in the load as the electrons return to emitter potential. The principles of operation and examples of applications are described in the literature.[1–3]

Higher efficiencies and lower material costs will be required in order to make combustion-heated TECs commercially viable. For this purpose, we suggest utilizing plasma-sprayed tungsten as emitter material instead of tungsten produced by chemical vapor deposition. The efficiency of a TEC can be increased by electrolytical etching the emitter surface.[4] The higher efficiency was attributed to the production of {110} lattice planes as a result of the etching process.[4] It is known that {110} lattice planes of bcc metals have high bare work functions and low cesiated work functions. This results in high converter efficiency.[5]

Some experiments with an etched and an unetched emitter will be described in order to show the increased efficiency and how it is obtained. Measurements of the current-voltage (I-V) characteristics were performed with a research diode. A sketch of this diode is presented in Fig. 1. The various parts of the diode were interconnected with stainless-steel flanges joined by copper gaskets. The diode was put in an evacuated bell jar for protection against corrosion by air. In order to outgas the diode, it was evacuated by a turbomolecular pump. For the ultimate vacuum (10^{-8} mbar) an AEI triode iongetter pump (120 ℓ/s) was used. More details of this research diode can be found elsewhere.[3,6]

II. THE ELECTRODE MATERIALS

A. The plasma-sprayed tungsten emitter

First, the features of the tungsten emitter will be described. A tungsten plate was produced by plasma spraying. According to the supplier (H. C. Starck, Berlin), the purity of the tungsten spraying powder was better than 99 wt %, and the C content was less than 0.05 wt %. After the spraying process the tungsten was reduced in a hydrogen atmosphere at a temperature of 1000 °C. Subsequently, the plate was sintered in a vacuum at 2000 °C.[7,8] A disk, 13 mm in diameter and 1 mm thick, was spark-machined from the plate. In order to degrease the disk, it was rinsed with freon. After drying it was rinsed with ethanol and distilled water. The tungsten disk was investigated by x-ray diffraction, scanning electron microscopy (SEM), and Auger electron spectroscopy (AES) analysis techniques, and found to be pure, texture-free tungsten. This disk was joined to the molybdenum emitter substructure of the research diode by vacuum brazing. Mo-42 at.% Ru was used as filler material. In the research diode the tungsten emitter faces a molybdenum collector. The distance between the two electrodes is variable between 0.01 and 1 mm.

After a number of experiments, the emitter surface was electrolytically etched for 50 s at a voltage of 2 V in a 3% NaOH aqueous solution. The same collector faced both the etched and the unetched tungsten emitter.

After the experiments in the research diode, the tungsten emitter was analyzed again with x-ray diffraction, SEM, and AES analysis techniques. A SEM picture of the emitter surface after the experiments is presented in Fig. 2. Grain boundaries can be seen. No macroscopically flat planes are present after the experiment. After some Ar^+

 0021-8979/90/161883-07$03.00

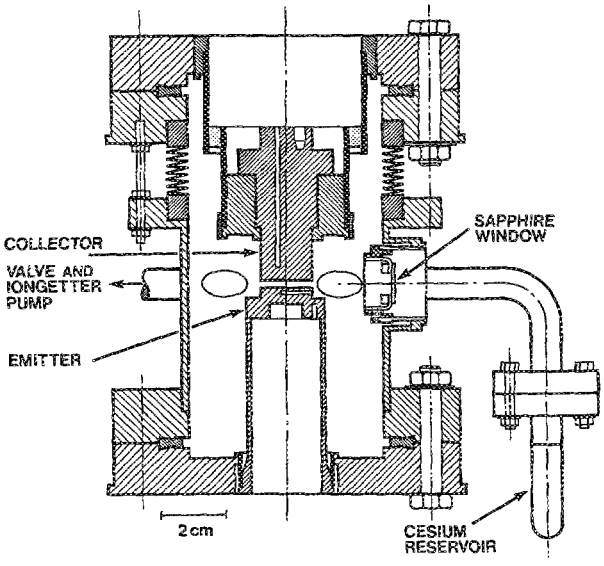

FIG. 1. Sketch of the research diode. The emitter is made of plasma-sprayed tungsten. The collector is made of molybdenum.

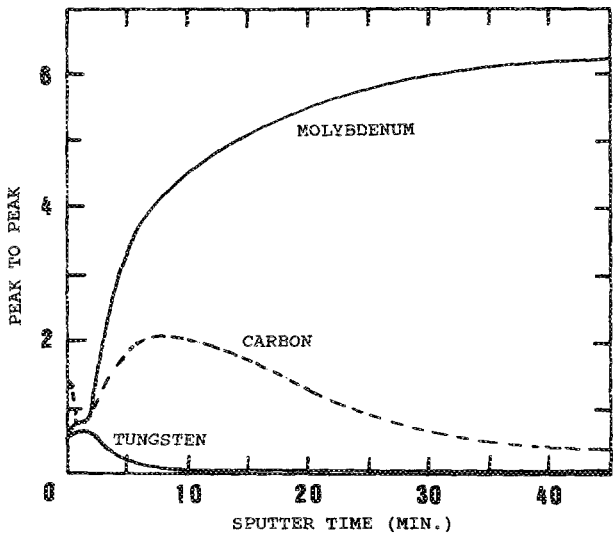

FIG. 3. Ar-ion sputter (5 keV, 30 μA/cm^2) depth profile of the collector surface after use in the research diode. AES signals of tungsten, molybdenum, and carbon are indicated.

sputtering in the AES apparatus, only very small amounts of carbon and oxygen were detected[7] on the emitter surface.

B. The molybdenum collector

The collector was machined from an arc-cast polycrystalline molybdenum bar. The molybdenum was of ABL2, low carbon, quality. According to the supplier (Amax Inc.), the C content was 0.003 wt %. In order to degrease the collector surface, it was rinsed with freon. After drying it was rinsed with ethanol and distilled water. After the experiments in the research diode, the collector surface was thoroughly investigated with x-ray diffraction, SEM, and AES analysis techniques.[7]

Carbides were detected with x-ray diffraction. It is difficult to discriminate between W_2C and Mo_2C by x-ray diffraction. However, since the temperature of the collector has not been higher than 700 °C, and W_2C is only stable above 1250 °C, it can be concluded that only Mo_2C is present on the collector surface.

The collector surface was also investigated in a SEM equipped with an energy dispersive x-ray (EDX) analyzer. Tungsten was detected on the surface of the molybdenum collector. The EDX analyzer was provided with a Be window, and so the carbon content could not be investigated. By the use of various acceleration voltages for the electron beam, it was found that a thin tungsten layer was deposited on the molybdenum surface. From the relative x-ray intensities at various acceleration voltages, the layer thickness was calculated. [9] Taking only the W-L radiation into account, and omitting the Mo-L radiation of the substrate, a tungsten layer thickness of 0.028 μm could be found. Also, AES analysis was used to examine the collector surface. An Ar^+-ion sputter depth profile of the Mo surface is presented in Fig. 3. After sputtering for 1 min, the superficial contamination from the air was removed, and it was seen that a thin W layer and a layer with C (Mo_2C) were present. If it is assumed that W is sputtered away as fast as Mo, then a Mo_2C layer thickness of about 0.3 μm is found. This value agrees with the relative intensities of Mo_2C and Mo found in the x-ray diffraction pattern of the collector surface. The description of the surface layers of the collector is therefore the following: On the molybdenum substratum a layer of 0.3-μm Mo_2C has grown, and the carbide is covered with a 0.028-μm-thick W layer, resulting from evaporation of the tungsten emitter. This configuration is confirmed by both the W-L and the Mo-L x-ray intensities measured in the SEM (EDX). Carbon shows no surface segregation in tungsten, and so it is expected that during the experiments in the research diode, the outer surface of the collector consisted of tungsten atoms. During the AES analyses, Ar^+-ion depth profiles were determined for O, Cs and Si.[7] In the W layer an increased oxygen content was found.

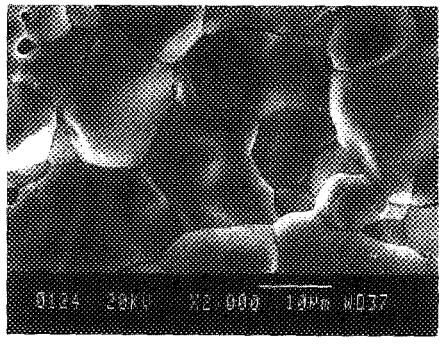

FIG. 2. SEM image of the tungsten emitter surface after use as an etched emitter. The bar corresponds to a distance of 10 μm.

III. WORK FUNCTION

A. Bare work function of the tungsten emitter

During the outgassing procedure, the electron emission current was monitored. At the ultimate emitter temperature (1640 °C), the total pressure in the research diode was 1.2×10^{-8} mbar. It is supposed that water molecules are the most unruly gas molecules to remove from the diode. The ultimate pressure in the diode is thus mainly due to water molecules. The partial oxygen pressure is estimated to be 3×10^{-9} mbar.

The effective work function of the electrode (Φ) is calculated from the saturation current density (I_s in A/cm^2) using the modified Richardson equation:

$$\Phi = kT_e \ln(120T_e^2/I_s), \tag{1}$$

where T_e is the emitter temperature in K and k is the Boltzmann constant. At two temperatures and at a small interelectrode distance (0.05 mm), a bare work function of 4.5 eV was calculated for the unetched tungsten emitter, whereas for the etched tungsten emitter a bare work function of 4.8 eV was found.

B. Work functions of the emitter and collector in a cesium atmosphere

In the unignited ion-rich mode, I-V characteristics were measured at various emitter temperatures (see Fig. 4). The interelectrode distance was kept small (0.05 mm) during these measurements. It is seen in Fig. 4 that saturation of the emitter emission current density occurs within the depicted voltage range. The cesiated work function of the tungsten emitter is calculated, at each cesium reservoir temperature, from the saturation current density using Eq. (1).

The Boltzmann line is indicated in Fig. 4. This line represents the equation:

$$I = 120T^2 \exp(V/kT_e), \tag{2}$$

where V is the voltage across the diode. The Boltzmann line depends only on the emitter temperature. The line describes the current density of the electrons which can cross a potential V if there are no other obstructions present. To obtain the Boltzmann line within the depicted voltage range, the line is shifted by 1.5 V. The voltage difference between the Boltzmann line and the actual measured I-V characteristic in the retarding range represents the voltage drop in the collector: i.e., the collector work function. From the characteristics depicted in Fig. 4, values for the work functions of the collector surfaces which face the etched and unetched emitter are found: $\Phi_c = 1.52$ and 1.70 eV, respectively, both of them at $T_c/T_{Cs} = 1.42$, where T_c and T_{Cs} are the absolute temperatures of the collector and the cesium reservoir.

As indicated in Sec. II B, the surface of the molybdenum collector facing the emitter also consists of tungsten. Figure 5 shows the work function of tungsten electrode

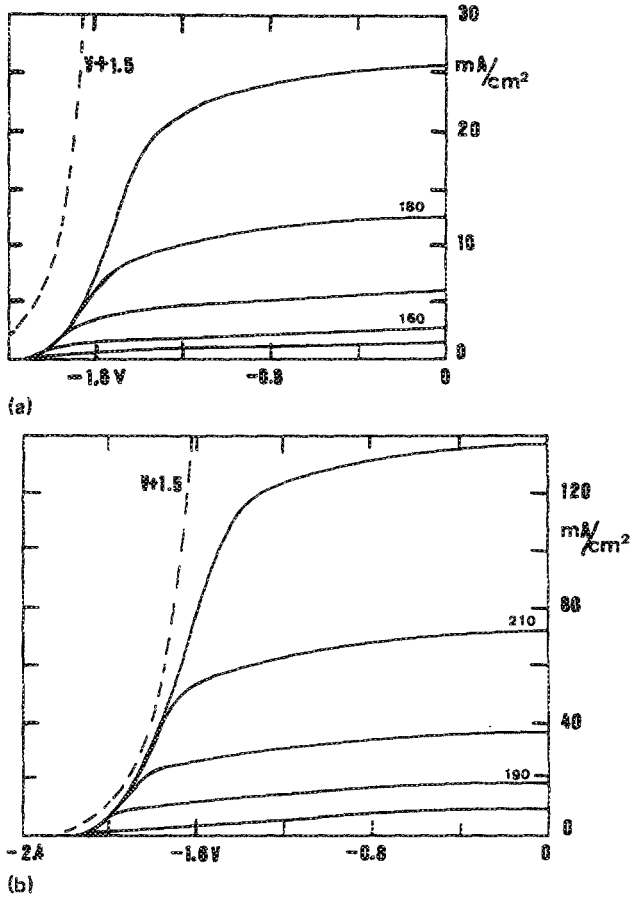

FIG. 4. Electron emission of the tungsten emitter in a cesium atmosphere. The experimental conditions correspond to an ion-rich unignited mode. The cesium reservoir temperature is indicated in °C (step 10 °C). The interelectrode distance is 0.05 mm. The dashed line is the Boltzmann line ($V+1.5$). In (a) the I-V characteristics of the unetched emitter are presented. The emitter and collector temperatures were 1300 and 354 °C. In (b) the characteristics of the etched emitter are presented. The emitter and collector temperatures were 1400 and 420 °C.

surfaces at both emitter and collector conditions. It is convenient to plot the work function on a reduced temperature scale. The reduced temperature is the ratio of the electrode temperature and the cesium reservoir temperature, both in K. Such so-called Rasor plots for etched and unetched tungsten are presented in Figs. 5(a) and 5(b). It is seen in Fig. 5 that the measured work function of plasma-sprayed tungsten deviates up to 0.1 eV from the values for tungsten given by Rasor and Warner.[10] Moreover, it is found that the cesiated work functions of the etched and unetched tungsten are identical within 0.05 eV. The cesiated work functions of the etched emitter at 1200 °C were measured immediately after the emitter bare work function measurement at 1400 °C. The cesiated work functions of the etched emitter at 1200 °C are substantially lower (0.3 eV) than the cesiated emitter work functions measured for the unetched emitter. This 0.3-eV lower cesiated work function corresponds with the 0.3-eV higher bare work function. However, the low cesiated emitter work function of the etched emitter disappears at temperatures higher than 1200 °C.

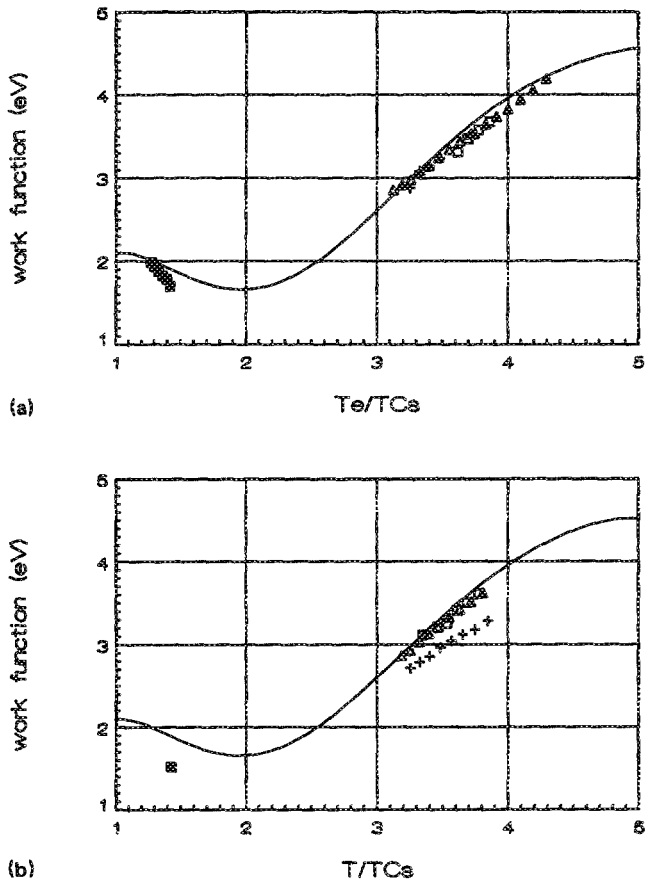

FIG. 5. The work function of the tungsten emitter calculated from the saturation current density measured in the ion-rich unignited mode (see Fig. 4). The curve represents the work function of polycrystalline W as given by Rasor and Warner (Ref. 10). The work functions of the unetched and etched emitter are presented in (a) and (b), respectively. Various emitter temperatures were used: + : 1200; △: 1300; □: 1400; and ▲: 1500 °C. In (a) and (b) also the work functions of the tungsten film deposited on the molybdenum collector are indicated, which are measured in the retarding range of the unignited ion-rich mode (▩) (see Fig. 4 and Ref. 7).

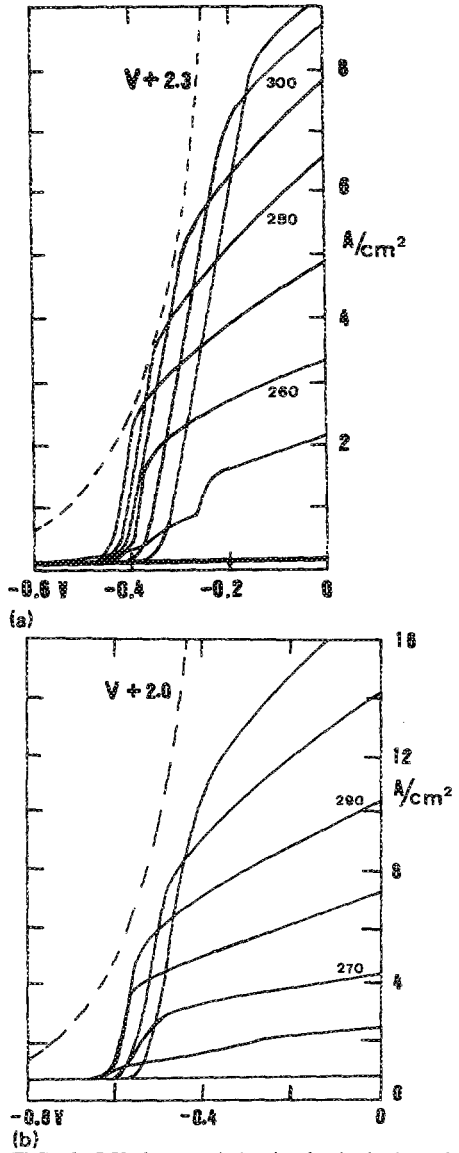

FIG. 6. *I-V* characteristics in the ignited mode. The cesium reservoir temperature is indicated in °C. The emitter and collector temperatures are 1400 and 630 °C, respectively. The interelectrode distance is 0.3 mm. The dashed line is the Boltzmann line (a: $V+2.3$ V, b: $V+2.0$ V). In (a) the characteristics of an unetched emitter are presented. In (b) the characteristics of an etched tungsten emitter are shown.

IV. THE IGNITED MODE

A. The dependence of the *I-V* characteristics on the cesium reservoir temperature

At higher cesium reservoir temperatures and larger interelectrode distances, the cesium vapor in the diode ignites, and a plasma is created in the interelectrode space. Higher currents are generated by the diode. To avoid the effects of the electrical resistance of the leads, the *I-V* characteristics are measured using a four-point method.[6] The characteristics are obtained with a Tektronix 577 D2 curve tracer with sense connection using alternating voltage (50 Hz). Various *I-V* characteristics were measured keeping the emitter temperature, the collector temperature, and the interelectrode distance constant and varying the cesium reservoir temperature. It is seen in Fig. 6 that there is an optimum cesium reservoir temperature. At a lower cesium reservoir temperature, the voltage across the diode is higher, because the resistance of the cesium plasma is lower. However, a lower cesium reservoir temperature results in a higher emitter work function and thus in a lower current.

In Fig. 6 the Boltzmann line is again indicated. At the conditions prevalent a plasma is present in the diode. There are two processes by which the electrons lose energy: (1) by entering the collector (Φ_c) and (2) by interactions in the plasma (V_d). These two losses determine the voltage difference between the Boltzmann line and the actual measured *I-V* characteristic in the retarding range. This voltage difference is called the barrier index (V_b):

$$V_b = \Phi_c + V_d, \tag{3}$$

and it characterizes the performance of any real thermionic converter. The lower the barrier index is, the higher the performance of the converter. The lowest barrier indexes realized up until now are $V_b = 2.0$ eV.[1] It is seen from Fig.

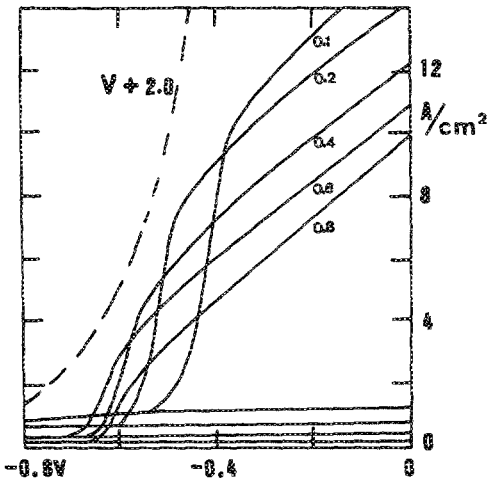

FIG. 7. The influence of the interelectrode distance (indicated in mm) on the *I-V* characteristics of a diode with an etched tungsten emitter. The emitter, collector, and cesium reservoir temperatures were 1400, 630, and 300 °C, respectively.

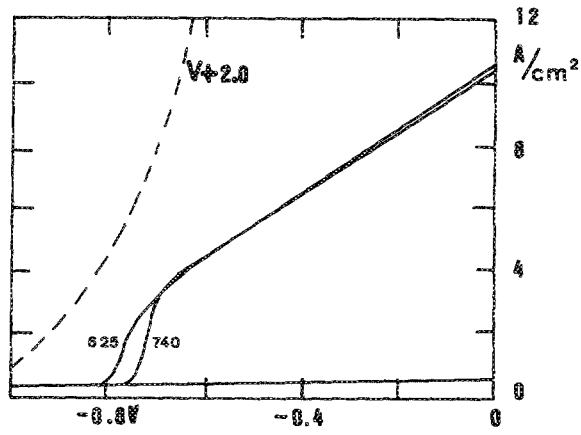

FIG. 8. The influence of the collector temperature (indicated in °C) on the *I-V* characteristics of a diode with an etched tungsten emitter. The emitter and cesium reservoir temperatures were 1500 and 310 °C, respectively. The interelectrode distance was 0.4 mm.

6 that the value of the barrier index depends on the current density at which it is determined. If not stated otherwise, we take the lowest barrier index, which is the barrier index at the knee of the *I-V* characteristic. At this point the electrical power density is the highest. The values for the barrier indexes obtained for the diodes with an etched and an unetched tungsten emitter are then $V_b = 2.06$ and 2.30 eV, respectively.

B. The dependence of the *I-V* characteristics on the interelectrode distance

After the measurement of a family of *I-V* characteristics at various cesium reservoir temperatures, the conditions in the research diode were systematically changed. First, the interelectrode distance was changed in the range from 0.1 to 0.8 mm. Next, the collector temperature was changed and ultimately the emitter temperature was changed. In Fig. 7 the influence of a changing interelectrode distance is presented. It is seen that a smaller interelectrode distance results in a higher current density, but the barrier index increases too. The current in the unignited mode increases too as the interelectrode distance decreases. If the voltage across the diode is considered at a constant current density (e.g., 8 A/cm^2), it is seen that a maximum occurs in the dependence of the voltage on the interelectrode distance. This maximum can be qualitatively explained by the competition of two processes: ion generation and elastic scattering. At small spacings ion generation is inadequate and hence limits the flow of electrons. At large spacings ion generation is plentiful, but elastic scattering collisions are so frequent that they predominate and limit the flow of electrons.

C. The dependence of the *I-V* characteristics on the collector temperature

The influence of the collector temperature is presented in Fig. 8. It is seen that the *I-V* characteristics are not very sensitive to variations in the collector temperature; a difference of 100 °C in the collector temperature hardly influences the current density. In principle, the collector temperature can influence the *I-V* characteristic in two ways: (1) It changes the collector work function and, therefore, the electrode voltage according to the equation

$$e\Delta V = \Delta\Phi_c, \tag{4}$$

and (2) it influences the collector emission according to the Richardson equation. For low collector temperatures the collector emission is negligible; therefore, the collector temperature affects only the output voltage according to Eq. 4. For high collector temperatures back emission is no longer negligible, and an increase in collector temperature results in an increase in reverse current; this tends to reduce the converter output power.

D. The dependence of the *I-V* characteristics on the emitter temperature

An example of the influence of the emitter temperature on the *I-V* characteristic is shown in Fig. 9. Collector and cesium reservoir temperatures as well as the interelectrode distance are the same at both emitter temperatures. At the lower emitter temperature and at a low output voltage, the current density is higher. This is caused by the lower emitter work function at the lower emitter temperature. The work function is lower because the cesium desorption rate at the emitter surface is smaller. If the current at the knee in the *I-V* characteristic is supposed to be half the saturation current, then, using the measured work functions of Fig. 5, the same currents are obtained, both calculated and observed. They are 5 and 4 A/cm^2 at, respectively, 1400 and 1500 °C. From the slope of the characteristics at low output voltage, it is seen that the Schottky effect is greater in case of the low emitter temperature. At an elevated emitter temperature, the maximal output voltage is higher because the emitted electrons have a larger kinetic energy. If the difference in kinetic energy were the only effect, a

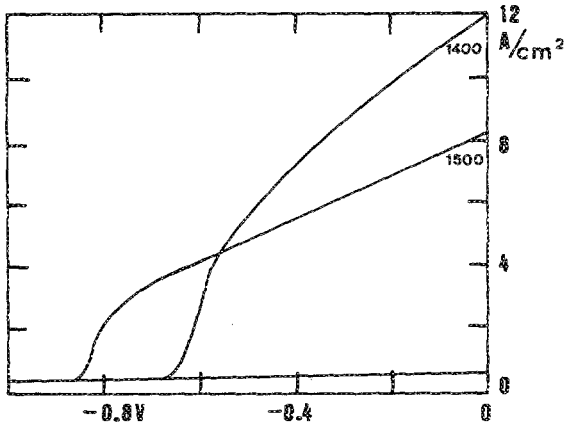

FIG. 9. The influence of the emitter temperature (indicated in °C) on the *I-V* characteristics of a diode with an etched tungsten emitter. The collector and cesium reservoir temperatures were 630 and 300 °C, respectively. The interelectrode distance was 0.4 mm.

voltage difference of $\Delta V = 2k\Delta T_e = 0.017$ eV would be expected.[2] However, as can be seen in Fig. 9, experimentally the difference is ten times higher. This is caused by the fact that the larger kinetic energy of the electrons also changes the ionization and recombination processes in the plasma, resulting in a lower cesium plasma resistivity.

E. The electrical power density

The electrical power density (P, in W/cm^2) generated by the converter can be calculated from the *I-V* characteristics simply by multiplying a fixed voltage and measured current density at this voltage. At the conditions of Figs. 6(a) and 6(b), power densities of 1.5 and 4.5 W/cm^2 are found for the diode with the unetched and etched tungsten emitter. Thus the generated electrical power of the diode with the etched emitter is three times higher than the power generated by the converter with the unetched emitter. An example of the power density at various interelectrode distances is given in Fig. 10. A maximal power density is obtained at a 0.2-mm interelectrode distance.

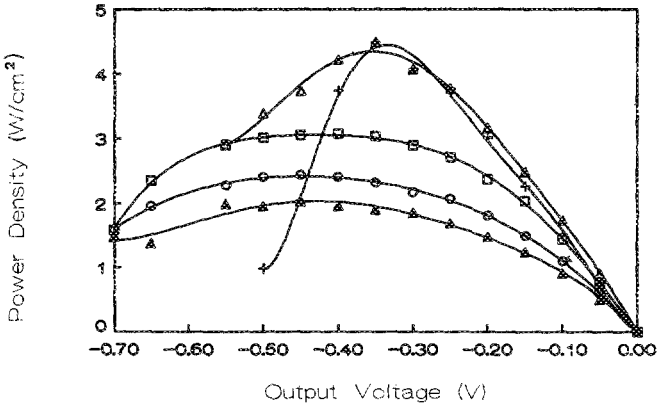

FIG. 10. The power density of a diode with an etched tungsten emitter at various interelectrode distances: + : 0.1; △: 0.3; □: 0.4; ○: 0.6; and ▲: 0.8 mm. The emitter and collector temperature were 1400 and 630 °C, respectively.

It is possible to estimate the efficiency of the converter (η) using the equation[2]

$$\eta = P/[(I/e)(\Phi_e + 2kT_e) + \sigma\epsilon(T_e^4 - T_c^4)], \qquad (5)$$

where e is the charge of an electron, ϵ is the effective thermal emissivity, and σ is the Stefan–Boltzmann coefficient. The efficiency depends strongly on the effective thermal emissivity, which value is the least known. We shall take a value $\epsilon = 0.2$ for the effective thermal emissivity.[6] At 1400 °C emitter temperature and optimized conditions ($T_c = 630$ °C, $T_{Cs} = 310$ °C, $\Phi_e = 2.4$ eV, $I = 12$ A/cm^2, and $V = 0.4$ V), an efficiency $\eta = 12\%$ is calculated.

V. DISCUSSION AND CONCLUSIONS

The aim of research in thermionic energy conversion is to gain an efficiency as high as possible. However, the efficiency strongly depends on impurities on the emitter and collector surfaces. It is well known that a small amount of oxygen increases the electrical power density of the converter.[1] At experimental conditions it is almost unavoidable that various impurities are present. Especially the collector surface is apt to be covered with impurities because it faces the hot emitter. Evaporated atoms from the emitter condense on the collector surface and influence the collector work function. As indicated in Sec. II B, the collector surface consists of W, whereas the collector body was made of Mo. Moreover, beneath the 0.03-μm-thick W layer, a 0.3-μm-thick Mo_2C layer had grown. Organic solvent cleaning (freon and ethanol) of the collector is suspected to be the carbon source for the Mo_2C layer. The outermost surface will determine the work function of the collector. Experimentally, it is not possible to detect significant differences between the work functions of a collector of pure polycrystalline Mo or W at unignited mode conditions ($T_c/T_{Cs} = 1.6$).[1,10] We have tried to measure the back emission of the diode,[7] but we do not trust the work function calculated from this current. Because there are no guard rings present in our diode, the measured back emission current will be too high.

We measured the collector work function in the retarding range[7] and found values in the same range as Gunther[1] (see Fig. 5). The collector work function is also evaluated from the emission current in the retarding range of the unignited mode, as given in Figs. 4(a) and 4(b). The values found for the collector work functions are $\Phi_c = 1.52$ and 1.70 eV ($T_c/T_{Cs} = 1.42$) for, respectively, the etched and unetched emitter case, which indicates a 0.18-eV lower work function for the collector which faced the etched emitter.

I-V characteristics, at equal experimental conditions, of the etched and unetched emitter are compared in Fig. 11. It is found that both the current and the voltage are higher in the etched case. The higher voltage across the diode can be traced back to the lower collector work function in the etched case. The 0.18-eV lower collector work function in the etched case corresponds with the approximately 0.2-V higher output voltage [see Eq. (4)]. It is seen

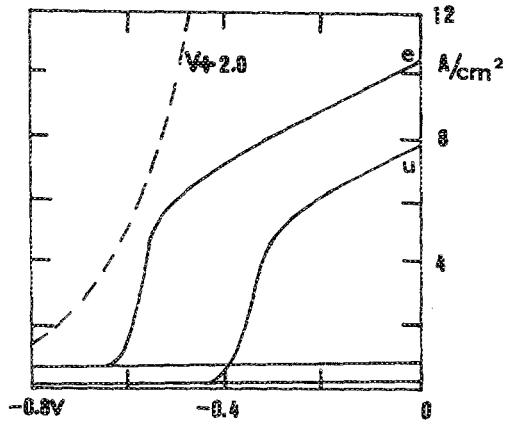

FIG. 11. A comparison of the characteristics of the diode with the etched (e) and unetched (u) emitter. The emitter, collector, and cesium reservoir temperatures were 1400, 630, and 290 °C, respectively. The interelectrode distance was 0.3 mm.

that the slope of the *I-V* characteristic is the same in the saturation region of both the etched and unetched emitter. If the *I-V* characteristic is shifted 0.2 V and the slope remains the same in the saturation region, a higher current density results. It is seen that the current density at the knee of the *I-V* characteristic of the etched emitter is only a little higher.

This higher current can be explained by a slightly lower emitter work function ($\Delta\Phi = 0.02$ eV) for the etched emitter. This difference is within the measurement accuracy of the work function measured from the unignited mode emission [see Figs. 4(a) and 4(b)]. The cesiated etched emitter is expected to be lower because some {110} tungsten crystal lattice planes are exposed at the surface. From the barrier indexes (V_b=2.06 eV for the diode with the etched and $V_b = 2.30$ eV for the diode with the unetched emitter) deduced in Sec. IV A, a plasma voltage drop can be deduced by using Eq. (3). If it is accepted that the work function of the collector depends on the reduced collector temperature (T_c/T_{Cs}) as indicated in Fig. 5, then the collector work functions at optimized condition ($T_c/T_{Cs} = 1.6$) are $\Phi_c = 1.6$ and 1.4 eV, respectively. The plasma voltage drop then has a value of about 0.7 eV in both cases, etched and unetched.

From the experiments we conclude that etching the emitter of a converter lowers the cesiated work function of the emitter only a little (about 0.02 eV). The maximal possible lowering is much larger, namely, the difference between the bare work function of a {110} tungsten lattice plane and a polycrystalline tungsten surface: $\Phi_{\{110\}} - \Phi_{poly} = 0.8$ eV.[1,2] The measured difference in bare work function was 0.3 eV. This difference can be explained by assuming that only a part of the surface area exposes {110} planes and that at high temperatures (1400 °C) the surface starts to roughen again. However, the effect of a change of the emitter temperature from 1200 to 1300 °C [see Fig. 5(b)] on the cesiated work function is hard to explain with these assumptions. Besides, from the *I-V* characteristics in the ignited mode, only a slightly lower cesiated work function ($\Delta\Phi = 0.02$ eV) for the etched emitter was deduced. A more plausible explanation is that during the electrolytical etching process, oxides are formed on the emitter surface. During the "bare" work function measurement, the oxides evaporate and only part of a monolayer of oxygen remains on the tungsten emitter surface. The result is an increased "bare" work function compared with the unetched emitter. At low emitter temperatures a stable Cs/O complex can be formed on the tungsten surface because the "2D oxide" structure on tungsten is not destroyed by cesium.[11] However, at 1300 °C the Cs/O complex is no longer stable, and Cs_2O evaporates from the emitter surface. As a result, the cesiated work function of the etched emitter at temperatures of 1300 °C and higher is only 0.02 eV lower than the work function of the unetched emitter.

In addition to the somewhat lower cesiated emitter work function ($\Delta\Phi = 0.02$ eV), the work function of the cesiated collector decreases substantially ($\Delta\Phi = 0.2$ eV). In our experiments the etched emitter was not outgassed before it was mounted in the research diode. During the outgassing of the etched emitter within the diode, oxides from the etched emitter may have condensed on the collector surface, causing the lowering of the cesiated collector work function. WO_3 is considered to be the evaporating oxide[12] during the outgassing and bare work function measurement procedures. Moreover, during the heating of the etched emitter—in a cesium atmosphere—in the temperature range from 1200 to 1300 °C, Cs_2O will have evaporated from the etched emitter. Besides, from the AES analyses an increased oxygen content was found in the condensed tungsten layer. The lower cesiated collector work function is considered to be the most important reason for the tremendous increase of electrical power density (factor of 3) found in the case where an etched emitter was used.

[1] G. N. Hatsopoulos and E. P. Gyftopoulos, *Thermionic Energy Conversion* (MIT, Camridge, MA, 1979), Vols. I and II.
[2] F. G. Baksht, G. A. Dyuzhev, and A. M. Martsinovskiy, *Thermionic Converters and Low Temperature Plasma*, English ed., edited by L. K. Hansen (Technical Information Center, Springfield, VA, 1978).
[3] G. H. M. Gubbels, L. R. Wolff, and R. Metselaar, Appl. Surface Sci. **40**, 193 and 201 (1989).
[4] V. C. Wilson and J. C. Danko, in *Conference Record of the 1969 Thermionic Conversion Specialist Conference*, Carmel, CA, edited by A. Schock (IEEE, New York, 1969), p. 46
[5] G. H. M. Gubbels and R. Metselaar, Surf. Sci. **226**, 407 (1989).
[6] G. H. M. Gubbels, L. R. Wolff, and R. Metselaar, J. Appl. Phys. **64**, 1508 (1988).
[7] G. H. M. Gubbels, Plasma Sprayed Tungsten as an Emitter for a Thermionic Energy Converter, Internal Report, ISBN 90-6819-011-3 (Eindhoven University of Technology, Eindhoven, 1989).
[8] G. H. M. Gubbels, Proceedings of the Thermionic Specialist Conference, edited by L. R. Wolff, ISBN 90-6808-019-9 (Eindhoven University of Technology, Eindhoven, 1989), p. 177.
[9] G. F. Bastin and H. J. M. Heijligers, Materialwiss. Werkstofftech. **21**, 90 (1990).
[10] N. S. Rasor and C. Warner, J. Appl. Phys. **35**, 2589 (1964).
[11] J. L. Desplat and C. A. Papageorgopoulos, Surf. Sci. **92**, 97 and 119 (1980).
[12] K. K. Schulze, H. A. Jehn, and G. Horz, J. Met. **40**, 25 (1988).